

Single-mode tellurite glass holey fiber with extremely large mode area for infrared nonlinear applications

Xian Feng*, Wei H. Loh, Joanne C. Flanagan, Angela Camerlingo, Sonali Dasgupta, Periklis Petropoulos, Peter Horak, Ken E. Frampton, Nicholas M. White, Jonathan H.V. Price, Harvey N. Rutt, and David J. Richardson

Optoelectronics Research Centre, University of Southampton, Southampton, SO17 1BJ, UK

**Corresponding author: xif@orc.soton.ac.uk*

Abstract: We report the fabrication of a large mode area tellurite holey fiber from an extruded preform, with a mode area of $3000\mu\text{m}^2$. Robust single-mode guidance at $1.55\mu\text{m}$ was confirmed by both optical measurement and numerical simulation. The propagation loss was measured as 2.9dB/m at $1.55\mu\text{m}$. A broad and flat supercontinuum from 0.9 to $2.5\mu\text{m}$ with 6mW output was obtained with a 9cm length of this fiber.

©2008 Optical Society of America

OCIS codes: (060.2280) Fiber design and fabrication; (060.5295) Photonic crystal fibers; (060.4370) Nonlinear optics, fibers

References and links

1. J. C. Knight, T. A. Birks, P. St. J. Russell and D. M. Atkin, "All-silica single-mode fiber with photonic crystal cladding," *Opt. Lett.* **21**, 1547-1549 (1996); Errata, *Opt. Lett.* **22**, 484-485 (1997).
2. P. Russell, "Photonic Crystal Fibers," *Science* **299**, 358-362 (2003).
3. T. M. Monro, Y. D. West, D. W. Hewak, N. G. R. Broderick and D. J. Richardson, "Chalcogenide holey fibres," *Electron. Lett.* **36**, 1998-2000 (2000).
4. T. M. Monro, K.M. Kiang, J. H. Lee, K. Frampton, Z. Yusoff, R. Moore, J. Tucknott, D. W. Hewak, H. N. Rutt and D. J. Richardson, "High nonlinearity extruded single-mode holey optical fibers," OFC2002 (OSA, Washington, DC, 2002), Postdeadline FA1, 1-3, (2002).
5. J. Y. Boniort, C. Brehm, PH. DuPont, D. Guignot, C. Le Sergent, "Infrared glass optical fibers for 4 and 10 micron bands," *Proc. 6th ECOC York (London: IEE, 1980)* 61-64 (1980).
6. J. S. Wang, E. M. Vogel and E. Snitzer, "Tellurite glass: a new candidate for fiber devices," *Opt. Mater.* **3**, 187-203 (1994).
7. T. M. Monro, D. J. Richardson, G. R. Broderick and P. J. Bennett, "Holey optical fibers: an efficient modal model," *J. Lightwave Technol.* **17**, 1093-1102 (1999).
8. X. Feng, T. M. Monro, V. Finazzi, R. C. Moore, K. Frampton, P. Petropoulos, D. J. Richardson, "An extruded single-mode high-nonlinearity tellurite glass holey fibre," *Electron. Lett.* **41**, 835-837 (2005).
9. T. Delmonte, M. A. Watson, E. J. O'Driscoll, X. Feng, T. M. Monro, V. Finazzi, P. Petropoulos, J. H. V. Price, J. C. Baggett, W. Loh, D. J. Richardson, D. P. Hand, "Generation of mid-IR continuum using tellurite microstructured fiber," CLEO/QELS Long Beach 21-25 May 2006 CTuA4 (2006).
10. P. Domachuk, N. A. Wolchover, M. Cronin-Golomb, A. Wang, A. K. George, C. M. B. Cordeiro, J. C. Knight, and F. G. Omenetto, "Over 4000 nm bandwidth of mid-IR supercontinuum generation in sub-centimeter segments of highly nonlinear tellurite PCFs," *Opt. Express* **16**, 7161-7168, (2008).
11. T. A. Birks, J. C. Knight, and P. St. J. Russell, "Endlessly single-mode photonic crystal fiber," *Opt. Lett.* **22**, 961-963 (1997).
12. A. M. Grassi, F. Casagrandea, M. D'Alessandro and S. Marinonia, "Single-modeness of short large mode area fibers: an experimental study," *Opt. Commun.* **273**, 127-132 (2007).
13. L. Dong, X. Peng, and J. Li, "Leakage channel optical fibers with large effective area," *J. Opt. Soc. Am. B* **24**, 1689-1697 (2007).
14. J. C. Baggett, T. M. Monro, K. Furusawa, V. Finazzi, D. J. Richardson, "Understanding bending losses in holey optical fibers," *Opt. Commun.* **227**, 317-335 (2003).
15. X. Feng, S. Tanabe, T. Hanada, "Hydroxyl groups in erbium-doped germanotellurite glasses," *J. Non-Cryst. Solids* **281**, 48-54 (2001).
16. X. Feng, S. Tanabe, and T. Hanada, "Spectroscopic properties and thermal stability of Er^{3+} -Doped germanotellurite glasses for broadband fiber amplifiers," *J. Am. Ceram. Soc.* **84**, 165-71 (2001).
17. G. Ghosh, "Sellmeier coefficients and chromatic dispersions for some tellurite glasses," *J. Am. Ceram. Soc.* **78**, 2828-30 (1995).

1. Introduction

Holey fibers (HFs), also known as photonic crystal fibers, have generated broad interest due to their unique guidance properties, such as the capability to exhibit photonic bandgaps, single-mode guidance in extremely large mode-area structures, high nonlinearity, strong birefringence, and dispersion management [1,2]. These optical properties are the result of a combination of the wavelength-scale features in the microstructured cladding and the large index contrast between the material and air. Following the work on silica holey fibers (HFs), high-index non-silica glass HFs have developed rapidly, offering advantages over silica HFs in the application areas of high nonlinearity optical fibers and low-loss mid-infrared transmission [3,4]. Non-silica glasses such as tellurite (i.e., tellurium dioxide TeO_2 based), fluoride and chalcogenide glasses have excellent optical transparency in the wavelength range of 0.5-5 μm , 0.4-6 μm and 1-16 μm respectively. In contrast, the transmission window of silica is limited to $< 3\mu\text{m}$. High-index non-silica glasses such as tellurites and chalcogenides also possess nonlinear refraction coefficients n_2 that are at least an order of magnitude higher than that of fluoride or silica. Furthermore, compared to fluoride and chalcogenide glasses, tellurite is much less toxic, more chemically and thermally stable, and hence is a highly suitable fiber material for infrared nonlinear applications [5,6].

Single-mode broadband supercontinuum (SC) sources ranging from 1 to 5 μm with medium power (mW-level) or high power (watt-level, or mW per nm of bandwidth) outputs are highly desirable for various applications including airborne light detection and ranging (LIDAR), optical coherence tomography (OCT), metrology, and IR spectroscopy. In order to efficiently convert the energy of the pump laser pulses to a continuum at new frequencies forming the continuum, the pump wavelength should be close to the zero dispersion wavelength (ZDW) of the fiber. Bulk tellurite glass has its ZDW at $\sim 2.1\mu\text{m}$, indicating that the first ZDW and the dispersion slope of the tellurite holey fiber can be tailored from short wavelengths to 2.1 μm through the use of holey fiber technology [7]. For efficient and compact all-fiber-based 1-5 μm SC devices, 1.5 μm (erbium doped) or 2 μm (thulium and/or holmium doped) pulsed fiber lasers represent attractive pump choices. Considering these aspects, tellurite holey fibers represent an attractive nonlinear medium for 1-5 μm SC devices.

We previously reported supercontinuum generated from 0.9 to 2.5 μm in a 20cm-length of single-mode tellurite holey fiber with a small effective mode area A_{eff} of 2.6 μm^2 , ZDW at 1.4 μm , using a femtosecond pulsed laser at 1.56 μm as the pump source [8,9]. A very recent work has demonstrated 1-5 μm SC from a 9mm-length of tellurite HF with a smaller A_{eff} of 1.7 μm^2 [10]. However, to scale the output SC power up to medium or high power levels, a nonlinear fiber with a larger mode area rather than small core fibers may be a more practical option, as the damage power thresholds of the former would be considerably higher. In this work, we demonstrate IR supercontinuum from a tellurite fiber with a mode area as large as 3000 μm^2 , pumped at 2.15 μm .

The tellurite holey fiber reported here is directly fabricated from an extruded preform, and has a core diameter of $\sim 80\mu\text{m}$. Robust single-mode guidance at 1.55 μm was confirmed by both optical measurement and numerical simulation. The fiber has an attenuation of 2.9dB/m at 1.55 μm and its ZDW is at 2.15 μm . We observe broadband SC between 1.0-2.5 μm using a 9cm length of this fiber, with 6mW output.

2. Fabrication

The tellurite glass has composition 75 TeO_2 -20 ZnO -5 Na_2O (mol.%) [6]. The glass has a refractive index of 2.0 and nonlinearity coefficient n_2 of $1.7 \times 10^{-19} \text{m}^2/\text{W}$ at 1.55 μm . A conventional melting-casting technique was used to make a glass billet with dimensions

32.8mm diameter and 36mm height. The billet was heated to the glass softening temperature (340°C) and extruded into a 125mm long preform. Figure 1(a) shows the cross-section of the extruded tellurite preform; 3 rings of holes surround a solid core. The preform has an outer-diameter (OD) of 15.9mm, hole diameter of 1.0mm, and hole-separation of 2.2mm. The preform was directly drawn into a few hundred meters of fiber with different ODs; the largest OD was $410 \pm 10 \mu\text{m}$. The total yield of the $410 \mu\text{m}$ OD fiber was 50 meters. Figure 1(b) shows an optical photograph of the cross-section of the fiber. It is seen that the fiber has a uniform hole spacing Λ of $53 \mu\text{m}$. Owing to effects such as temperature gradients in the radial direction, surface tension and residual air-pressure inside the holes during the fiber-drawing process, the average hole diameter d_i (i is the ring number counted from the core outwards, $i=1$ to 3) reduced from $d_1=28.1 \mu\text{m}$, $d_2=23.3 \mu\text{m}$, to $d_3=13.8 \mu\text{m}$, corresponding to d_i/Λ ratios of 0.53, 0.44 and 0.26 respectively. Note that the initial d/Λ ratio was 0.454 in the preform.

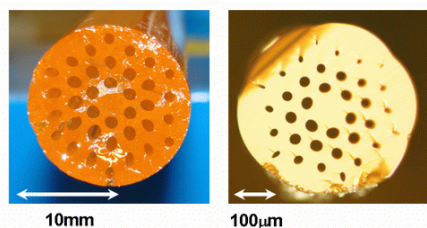


Fig. 1. Optical photographs of the cross-sectional views of (a) the extruded tellurite preform and (b) the resulting tellurite holey fiber with $410 \mu\text{m}$ OD.

3. Optical performance of the tellurite large mode area HF

In theory, for a holey fiber with an infinite cladding, an infinite number of rings of holes and hole-to-spacing ratio $d/\Lambda < \sim 0.4$, only the fundamental spatial mode can be allowed to propagate in the fiber. And this is true regardless of either the wavelengths or the core size. This is often referred to as the endlessly single-mode behavior of holey fibers [11]. In practice, for a HF with a finite number of air-filled holes, higher-order modes are likely to be observed, especially in a short length [12]. Increasing the differential loss between the fundamental LP_{01} mode and the higher order modes becomes the practical criterion for realizing effective single-mode operation [12,13].

The effective single-mode behavior of the fabricated tellurite large mode area (LMA) HF was first confirmed by numerical simulation. Figure 2(a) shows the simulated mode profiles of LP_{01} and LP_{11} modes at $1.55 \mu\text{m}$. The simulations indicate that the confinement losses of the fundamental mode (LP_{01}) and the first higher-order mode (LP_{11}) are $\sim 10^{-4} \text{dB/m}$ and $\geq 3 \text{dB/m}$ at $1.55 \mu\text{m}$, respectively. have Given the $\sim 10^{-4}$ ratio between the confinement losses of fundamental and the first higher order mode, the fundamental mode remains after a certain fiber length. In fact, in the range 1-5 μm , i.e., more than two octaves, the average ratio of the confinement loss of the LP_{01} mode to that of the LP_{11} mode is $\sim 10^{-4}$ (see Fig. 2(b)).

To observe the spatial mode guidance characteristics of the HF, the collimated beam from a pigtailed $1.55 \mu\text{m}$ laser diode (LD) was launched into the tellurite LMA HF. The launch objective (Edmund DIN4) has a NA of 0.1. The selection of a low-NA launch objective is important for the observation of single-mode guidance in our LMA HF. For a LMA HF, the high-order modes will easily be excited by using a high-NA launch objective and cannot be attenuated unless the fiber is strongly bent [12]. However, bending also increases the loss of the fundamental mode, and therefore our LMA HF of 1.5m length was kept straight. Robust guidance with a hexagonally symmetric mode profile was observed as shown in Fig. 3(a). An IR-Vidicon-camera (Hamamatsu, Model C2400-03, sensitivity range: 800-2100 nm) was used to take this image. This is in good agreement with the simulated fundamental (LP_{01}) mode (Fig. 3(b)). The beam quality factor M^2 was measured as 1.3 ± 0.1 , using a BeamScope-P5 (DataRay Inc.). The experimental results confirm that the fiber is effectively single-mode.

An effective mode area A_{eff} of $3000 \pm 200 \mu\text{m}^2$ was calculated for the fundamental mode LP_{01} , according to the numerical simulation. To our knowledge, this is the first report of such a large single mode area in a non-silica glass fiber - this is also comparable to the recorded LMA of $3160 \mu\text{m}^2$ recently reported by Dong et al in a silica holey fiber [13]. The effective nonlinearity γ ($\gamma = 2\pi n_2 / (\lambda \cdot A_{eff})$) of the tellurite LMA HF was calculated to be $0.23 \text{W}^{-1} \text{km}^{-1}$ at $1.55 \mu\text{m}$.

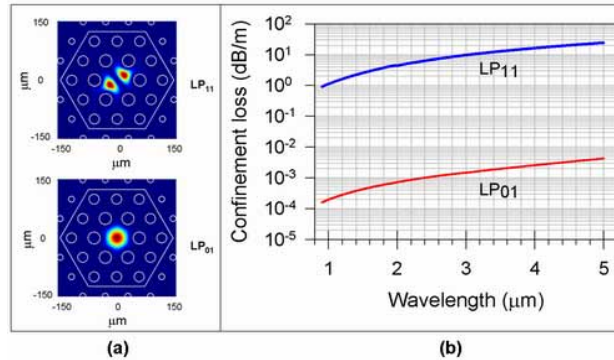


Fig. 2. (a). Simulated near-field mode profiles of the fundamental mode (LP_{01}) and the first higher-order mode (LP_{11}) of the tellurite LMA HF at $1.55 \mu\text{m}$; (b) Calculated confinement losses of LP_{01} mode and LP_{11} mode of tellurite LMA HF between $0.9\text{-}5.0 \mu\text{m}$

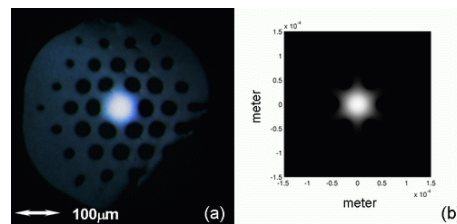


Fig. 3. (a). Observed guiding mode profile in tellurite LMA HF at $1.55 \mu\text{m}$; (b) simulated mode profile of fundamental mode (LP_{01}) of tellurite LMA HF at $1.55 \mu\text{m}$

In general, LMA fibers become increasingly bend-sensitive with increasing in mode area, because of the reduction in the effective numerical aperture (NA) of the fiber required to maintain single-mode guidance. This results in very weak confinement within the fiber [14]. The bend-induced loss on the LP_{01} mode in this fiber is estimated to be 0.3dB/m at a wavelength of $1.55 \mu\text{m}$ for a bend radius of 2m . The bend loss improves with longer wavelengths, e.g. at $2.0 \mu\text{m}$, the same loss (0.3dB/m) would occur at a bend radius of 1.3m . In addition, the higher-order modes are more sensitive to bend losses than the fundamental, which contributes in part to the observation of effective single-mode behavior in just 1.5m length of this fiber. The bend loss may be reduced further by increasing d/Λ [13] (i.e., increasing the hole size), but at the expense of reducing the loss discrimination between the fundamental and the higher order modes. From the current performance of this fiber, we expect that increasing d/Λ from 0.5 to 0.6 [13] would improve the bend sensitivity significantly while still retaining sufficient discrimination between modes.

4. Measured propagation losses

The cutback method was used to measure the propagation attenuation of this holey fiber at $1.55 \mu\text{m}$, using a pigtailed $1.55 \mu\text{m}$ LD as the source. The near-field image of the output end of the fiber was monitored by the IR-Vidicon-camera to ensure that the light was guided only in the fiber core. Figure 3(a) shows the guidance from the fiber at the starting length of 1.50m . The loss of $2.9 \pm 0.1 \text{dB/m}$ was linearly fitted at $1.55 \mu\text{m}$ from four cutbacks with a total cutback

length of 0.72m. For comparison, an unclad-unstructured fiber was also drawn from an extruded glass rod with the same composition. Figure 4 shows the spectrum of measured fiber attenuation of the unclad/unstructured fiber by the cutback method. A tungsten-halogen lamp with emission from 0.25-2.5 μm was employed as the broadband light source. An Ando optical spectrum analyzer and a monochromator with a cooled extended InGaAs photodiode were used to record the spectra between 0.6-1.6 μm and 1-2.5 μm respectively. One can see that at 1.55 μm , there is a $\sim 1.5\text{dB/m}$ loss increase for the LMA HF over that of the unclad-unstructured fiber. The attenuation of the unclad fiber with the same composition includes (i) the intrinsic material loss and (ii) the extrinsic loss arising from during the fabrication, such as the heat-induced crystallization, the impurities of transition metal ions and hydroxyl groups, (iii) the defects like bubbles, and so on. Since the LMA HF and the unclad fiber had very similar thermal history and fabrication process, from glass melting, extrusion, to fiber drawing, the enhanced attenuation of the LMA HF at 1.55 μm over the unclad fiber should be attributed to (i) the surface roughness inside the holes of the HF, (ii) some additional impurities involved into the preform during extrusion, and (iii) the bend-induced loss of the LMA HF. In addition, for the unclad fiber, the 1.4-1.5 μm band and 1.7-2.0 μm bands are due to overtone vibrations of hydroxyl groups remaining in the tellurite glass matrix [15].

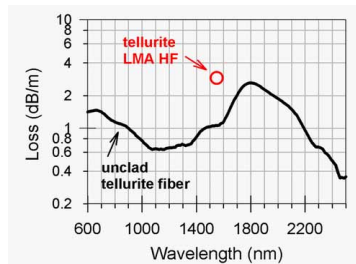


Fig. 4. Measured loss of tellurite LMA HF (the red dot) at 1.55 μm and the loss spectrum of unclad tellurite fiber (the black line)

5. Fiber dispersion and broadband infrared supercontinuum

The refractive index of the bulk tellurite glass (75TeO₂-20ZnO-5Na₂O (mol.%)) was measured using an ellipsometer from 400 to 1700 nm, as described in Ref. [16]. The dependence of refractive index n on wavelength λ was extended to 3 μm using the Sellmeier coefficients for a glass with the similar composition of 75TeO₂-25ZnO (mol.%) [17]. The material dispersion $D_m(\lambda)$ was then derived according to $D_m(\lambda) = -(\lambda/c) \cdot [d^2n(\lambda)/d\lambda^2]$. The total dispersion of the fiber is the sum of the waveguide dispersion D_w and material dispersion D_m . For the LMA HFs, the overall dispersion will approach the bulk material dispersion, since the waveguide dispersion becomes negligible in the limit of $A \gg \lambda$. A ZDW of 2.15 μm is therefore expected for this fiber (Fig. 5(a)). We note that although chalcogenide glasses have n_2 that are 2-3 orders of magnitude larger, the ZDW of bulk chalcogenide glasses is $>5\mu\text{m}$ [3]. Shifting the ZDW of a chalcogenide fiber from 5 μm down to 1.5 or 2 μm for efficient SC would require reducing the fiber core diameter to 1-2 μm , rendering such glasses less suitable for high power applications.

Broadband infrared SC from the fabricated tellurite LMA HF was obtained by pumping the fiber with 120fs laser pulses from an optical parametric amplifier (OPA). The pump wavelength was set at 2.15 μm , the ZDW of the fiber. The OPA was pumped by a regeneratively amplified Ti:sapphire laser operating at 1kHz (Coherent Opera pumped by Coherent Legend) at 800nm, and the idler beam launched into the tellurite LMA HF via a 0.1 NA microscope objective. A longwave pass filter (Thorlabs FEL1500) was placed before the objective to filter out residual signals from the OPA for wavelengths shorter than 1500nm. A neutral density filter was placed before the LMA HF, to allow us to observe the SC spectra at different values of average pump power P_{av} .

The light from the output end of the HF was butt-coupled to a 2-meter multimode fluoride glass fiber with 160 μm core diameter (GFF-160/200-230, Fiberlabs, Japan) and the SC spectrum was recorded by a monochromator with a cooled extended InGaAs photodiode. Since the multimoded fluoride fiber has losses of <0.1dB/m between 0.5-3.8 μm , it does not distort the generated spectrum from the tellurite HF. Figure 5(b) shows the SC generated in a 9cm long tellurite LMA HF. It can be seen that the SC broadens towards both shorter and longer wavelengths. The SC spectrum spans from 0.9 to >2.5 μm at the maximum P_{av} of 15.2mW, i.e., 15.2 μJ per pulse. Beyond 2.5 μm , the spectrum could not be measured due to the long-wavelength limit of the detector. The image of the SC signal at the output end of the LMA HF at the maximum P_{av} was captured by the IR-Vidicon-camera (see in Fig. 5(c)). It can be seen that most of the output is contained in the fiber core.

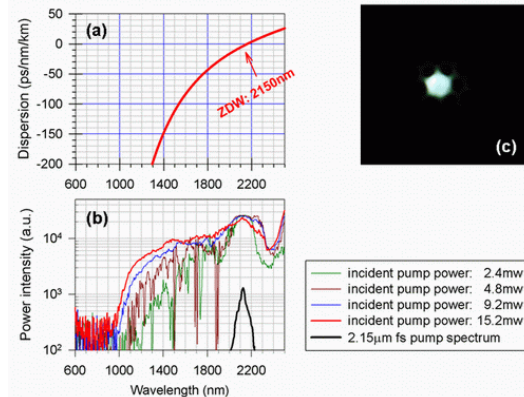


Fig. 5. (a). Dispersion profile of the tellurite LMA HF; (b) SC spectra from a 9cm long tellurite LMA HF under various launch input powers; (c) Observed near-field image of the HF with 6mW output SC spectrum under incident pump power of 15.2mW. Note that the incident pump power was measured before it was launched into the HF.

The SC power from the output end of HF was measured to be $6.0 \pm 0.2 \text{mW}$ at the maximum pump power. Note that the combined backward Fresnel reflection coefficient from both ends of the fiber is 20%, as the tellurite glass has a high index of 2.0. During the course of the SC measurements, no physical damage to the fiber facets was observed. It is somewhat surprising that self-focusing-induced damage does not occur in the fiber even under the MW-level peak pump power. While the reason(s) for this is still unclear, it may be that IR glasses such as tellurite and chalcogenides, with their smaller bandgap than silica, generate a low-density electron plasma more readily under strong optical excitation, thereby counteracting the self-focusing effect and preventing catastrophic optical damage [18].

6. Conclusions

In conclusion, we have successfully fabricated a very large mode area (3000 μm^2) tellurite holey fiber and shown effective single-mode guidance in it. The fiber has a propagation loss of 2.9dB/m at 1.55 μm and a zero dispersion wavelength at 2.15 μm . Broadband SC spectra extending from 0.9 μm to beyond 2.5 μm were generated in a 9cm long piece of the fiber, with a maximum output power of 6mW. The resistance to the high peak pump powers required for generating SC in this large mode area fiber suggests that the scaling to even higher average powers is likely to be viable, e.g. through further scaling up of the pulse repetition rate.

This work is funded by the Engineering and Physical Sciences Research Council (EPSRC) of United Kingdom, with a part contribution by BAE Systems (U.K.) and SELEX Sensors and Airborne Systems (U.K.). J. H. V. Price is supported by a Royal Academy of Engineering/EPSRC research fellowship.